WOOD RESEARCH doi.org/10.37763/wr.1336-4561/66.6.981994
e-ISSN 2729-8906
66(6): 2021 981-994 pp.

EFFECT OF EDGE DISTANCES ON STIFFNESS OF SHEAR-TENSION MODE IN GLULAM CONNECTIONS WITH INCLINED SCREWS

YIFAN LIU[1], ZIYIN YAO[1], FEIBIN WANG[1], HUI HUANG[2], ZELI QUE[1]
[1]NANJING FORESTRY UNIVERSITY
P.R. CHINA
[2]JIANGXI ACADEMY OF FORESTY
P.R. CHINA

(RECEIVED APRIL 2021)

ABSTRACT

The effects of edge distances on stiffness in glulam connections with inclined self-tapping screws were studied in this paper. Under four anchorage angles (A-45°, A-60°, A-75°, A-90°) and three edge distances (EG-2*D*, EG-4*D*, EG-6*D*) conditions, the shear-tension tests were carried out on the timber structure connections with inclined self-tapping screws, and the stiffness and other properties of the connections were tested. Based on the results, the effects of edge distances on stiffness in joints were quantified using the equivalent energy elastic-plastic (EEEP) model. The results showed that the edge distances had a certain impact on the yield mode and load-carrying performance of the joints. Within a certain range of variation, as the edge distance increased, the stiffness of the connections increased gradually, showing a positive correlation. The stiffness of specimen EG-2D is 4.41 kN·mm^{-1}. The stiffness of specimen EG-4D is 10.04 kN·mm^{-1}, which increases by 128% compared with the specimen EG-2D. The stiffness of specimen EG-6D is 12.08 kN·mm^{-1}, which increases by 174% compared with the specimen EG-2D. However, the ductility coefficient, yielding load, and energy dissipating have no significant change. Within a reasonable edge distance, only ductile damage occurred.

KEYWORDS: Inclined self-tapping screw, edge distances, edge distances, stiffness, glulam.

INTRODUCTION

Modern dowel-type fasteners, self-tapping screws (STS) have higher strength and stiffness compared with a traditional screw, which is widely used in mass timber structure (Blass and Bejtka 2001, Ringhofer et al. 2015) as shown in Fig. 1. This type of screw mostly features a continuous thread over the whole length (fully-thread) which leads to a more

uniform load transfer between the screw and the wood material (Dietsch et al. 2015, Jockwer et al. 2014). In recent years, many experimental (Yang et al. 2020, Zhang et al. 2019) and numerical studies (Brandner et al. 2018) concern about how the increase of screw inclination provides an increase of load-carrying capacity of the joints and concludes that is a significant change (Tomasi et al. 2010, Bejtka and Blass 2002, Wang et al. 2019, Komatsu et al. 2019, Yang et al. 2018, Que et al. 2020, Lu et al. 2020, Teng et al. 2020, Chen et al. 2020, Chang et al. 2019). Blass and Bejtka first clarified and proposed theoretical equations for the load-carrying capacity of inclined STS joint based on Johansen's theory (Johansen 1949). However, the inclined STS have more complex behavior in laterally loading condition which governed by the embedment behavior of the timber, withdrawal action on the screw and rope effect for large deformations. The assessment of the stiffness of the inclined STS has been studied by a few researchers (Girhammar et al. 2017, Symons et al. 2010, Tomasi et al. 2010).

Fig. 1: The engineering application of self-tapping screw.

According to Eurocode 5 (EN 1995-1-1, 2009), the slip modulus of the connector is depends on the timber properties and diameter of STS. It can be expressed as:

$$k_{ser} = \rho_m^{1.5} \cdot d/23 \quad (1)$$

$$k_{ser} = \rho_m^{1.5} \cdot d^{0.8}/30 \quad (2)$$

where: k_{ser} is the slip modulus of a connector for design at serviceability limit state ($N \cdot mm^{-1}$); ρ_m is the density of the timber ($kg \cdot m^{-3}$). The values of d mean the effective diameter of STS where the effective diameter is 1.1 times the thread root diameter (mm).

The Eq. 1 applies to nails without pre-drilling and Eq. 2 applies to screw. This equation can predict the stiffness of shear-compression stress in some cases. However, for the screws subjected to shear-tension stress, the equation is not able to accurately evaluate the stiffness. Therefore, Tomasi et al. (2010) further proposed the mechanic-based model to estimate the properties of STS connection. It can be expressed as:

$$k_{ser} = k_{\perp} \cdot cos\alpha \cdot (cos\alpha - \mu \cdot sin\alpha) + k_{\parallel} \cdot sin\alpha \cdot (sin\alpha + \mu \cdot cos\alpha) \quad (3)$$

where: $k_{\perp}$ is the connector stiffness for lateral loading; $k_{\parallel}$ is the connector stiffness for withdrawal loading; α is the angle of inclination of the STS; μ is the friction coefficient of the wood element.

According the Eq. 3 the stiffness of this connection can be seen by the two parts that lateral stiffness and the withdrawal stiffness of the screw. The lateral and withdrawal stiffness were affected of two parameters which is the interface friction of wood element and the inclined angle of the screw. As the angle changes, these two stiffnesses contribute differently to the overall stiffness of the connection. For example, the angle of inclination is 0°, the overall stiffness of the node is the vertical component of the screw, which is completely borne by the compressive bearing stiffness of the screw. This trend can also be reflected in the Fig. 2. The figure showed the stiffness for the screw subjected to shear-tension stress versus the inclination angle for the case where the friction coefficient has different value. The "willow leaf" enclosed area represents the node stiffness of the self-tapping screw subjected to shear-tension stress could appear possible area.

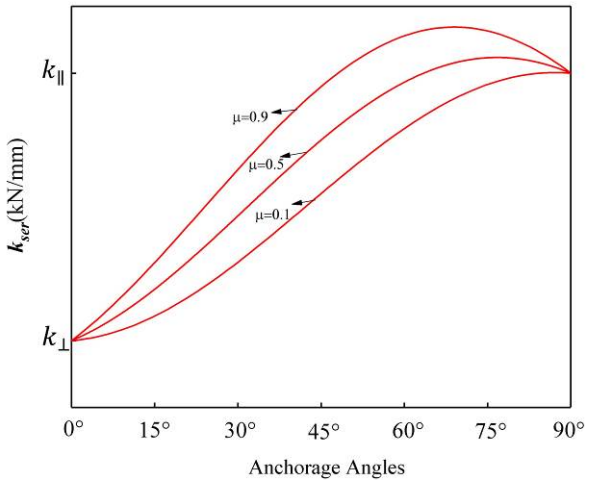

Fig. 2: The influence of the inclination (α) on the stiffness value.

Tomasi's model (Tomasi et al. 2010) is only a theoretical derivation model, but in actual engineering, the stiffness of self-tapping screws will change differently under the influence of different margins, end distances, and group effects.

The above research did not even address the edge distance effect of the stiffness for the STS. For the real project, the calculation formula given in the standard Eurocode 5 (EN 1995-1-1, 2009) has restrictions, the edge distances, end distances, and spacing lead to more complex mechanisms of the STS. This paper aims to introduce and experimentally verify the effect of edge distance on the stiffness of the timber structure joint connected with STS used the glulam material.

MATERIAL AND METHODS

Materials

The specimens were fabricated in factory that glulam made of Douglas fir (*Pseudotsuga menziesii*), of strength class SZ1 according to GB 50005-2017 (2017), and PUR adhesive (Polyurethane Reactive). The lamina of the glulam thickness was 35 mm. The average moisture content was 10.5%, and the average air-dry density was 0.538 $g \cdot cm^{-3}$. The manufacture of glulam processing with adhesive spread 250 $g \cdot m^{-2}$, compacting pressure 1.0 MPa, pressure time 4 h, processing temperature 25°C.

The self-tapping screws are FTLD (product number) cylindrical head with full thread structure. The diameter × length of self-tapping screws is 6 mm × 140 mm, as showing in Fig. 3 and Tab. 1. Withdrawal and bending tests carried out on the self-tapping screws in compliance with LY/T 2377-2014 (2014), LY/T 2059-2012 (2012), and ASTM F 1575-17 (2017), the average result of withdrawal strength is 25.79 $N \cdot mm^{-2}$, and the average bending yield strength is 1064 MPa.

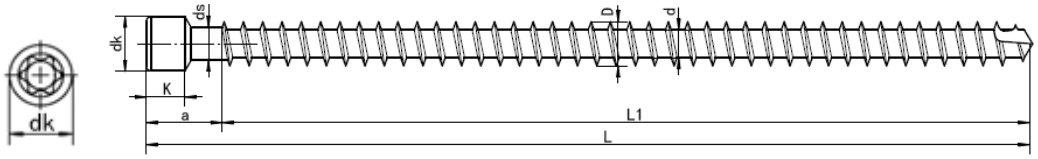

Fig. 3: FTLD self-tapping screw.

Tab. 1: The dimensions of FTLD self-tapping screw (units: mm).

Type	***L***	***L1***	***D***	***d***	***dk***	***K***
FTLD	140.0	130.0	6.0	4.0	8.4	5.5

The plan of the experiment

The specimen was designed by reference to the Chinese national standard GB 50005 2017 (2017) and the European standard Eurocode 5. The samples usually study in push-out tests, for example, it consists of two lateral wood (70 × 90 × 300 mm) elements and a central one (140 × 90 × 300 mm), held together by self-tapping screws: *(a)* The different anchored angle of single inclined self-tapping screws working only under shear-tension load (A-45°, A-60°, A-75°, A-90°); *(b)* The different edge distance of single inclined self-tapping screws working only under shear-tension load (EG-2*D*, EG-4*D*, EG-6*D*).

In the study, the influence of the screw angle, two self-tapping screws are screwed in from both sides of the lateral wood elements, the edge distance is 36 mm, the end distance is 108 mm, and the inclined angle is 45°, 60°, 75°, and 90° resp. To analyze the influence of the screw edge distance, were set to 2 *D* (12 mm), 4 *D* (24 mm), 6 *D* (36 mm), a total of three sets of specimens. The test was repeated six times for each group, and the test design was shown in Fig. 4.

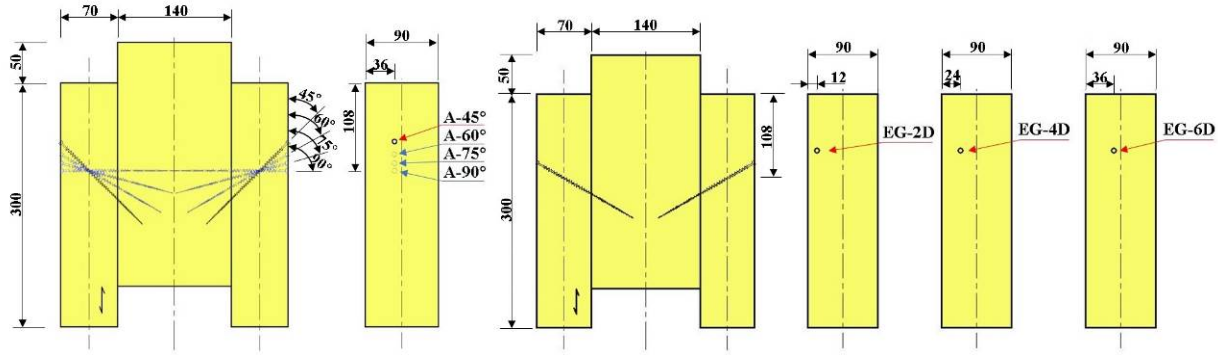

Fig. 4: The schematic plans of specimens with different angles and edge distances. Units (mm).

Test protocol and instruments

The protocol of the push-out test was referenced in American standard ASTM D1761-12 (2012) the deformation speed of the mechanical test machine was set 0.9 $mm \cdot min^{-1}$ (± 50%) by monotone displacement control of this test. Under this loading condition, the push-out test gets the maximum load within 5 - 20 min. During the experiment, when the load of the specimen has fallen to less than 80% of the maximum load, the loading is to stop, while using date collection system TDS-530, four linear variable differential transformer transducers (LVDT) and mechanical load sensor, acquisition of force and displacement data. The protocol of the loading is shown in Fig. 5.

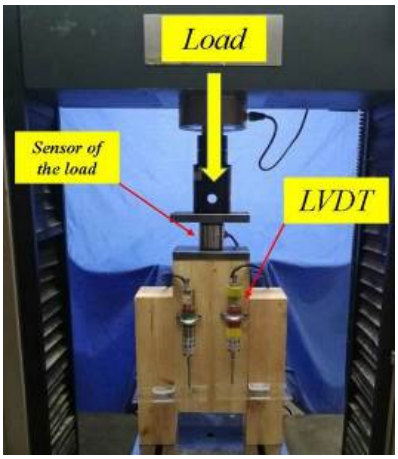

Fig. 5: Apparatus of the testing.

RESULTS AND DISCUSSION

Equivalent energy elastic-plastic method

The test results are shown in Fig. 6 and Fig. 7. It is significant to know the yield point when the plastic deformations occurred in seismic. In seismic design, plastic deformations are allowed for ductile structures. Therefore, it is important to know the yield point, when the plastic deformation begins, and ductility, how much plastic deformation the structure can undergo without significant loss of strength (Williams et al. 2008).

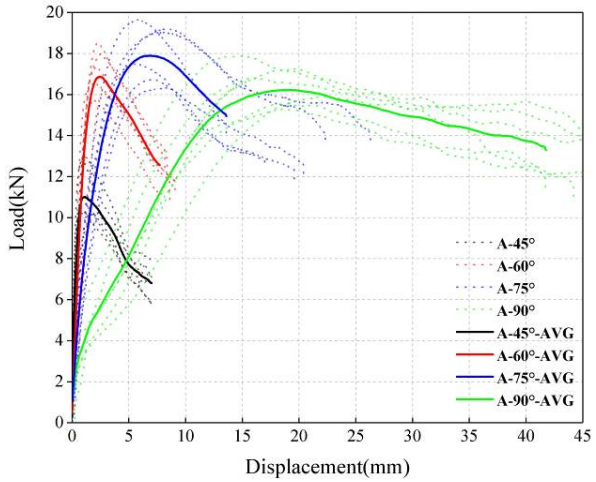

Fig. 6: The load-slip curves of specimens with different anchorage angles.

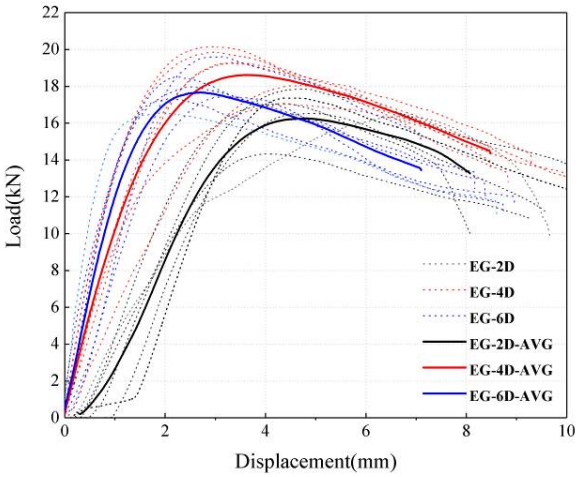

Fig.7: The load-slip curves of specimens with different edge distances.

There are several methods around the world to quantify these properties for timber structures. In this paper adopted the equivalent energy elastic-plastic (EEEP) curve method that usually analysis the shear walls in ASTM E2126-19 (2019). The bilinear curve represents the accurate elastic-plastic behavior of the connection. The area below the test curve is equal to the area under the bilinear curve. The initial stiffness defined by 0% and 40% of the maximum load. Deformation at failure is defined as the deformation at 80% of the maximum load. The yield load can be calculated using this following equation:

$$p_y = \left[\Delta_{failure} - \sqrt{\Delta_{failure}^2 - 2w_{failure}/K}\right] \times K \tag{6}$$

where: p_y is yield load; $\Delta_{failure}$ is deformation at failure; and $w_{failure}$ means energy dissipated until failure.

Then we can equivalent the test curve to the bilinear curve directly. The first line of the bilinear curve corresponds to the initial stiffness and yield load. Once the yield load is defined, the yield deformation can be determined. The ductility of the connection can be calculated.

Equivalent energy elastic-plastic analysis for different anchorage angles

As is shown in the Fig. 8, the load-slip curves and bi-linear models of specimens with different anchorage angles. The stiffness of the joint is the largest at 45°, and as the anchorage angle increases, the stiffness of the joint gradually decreases. That is consistent with the slope part of the bi-linear model.

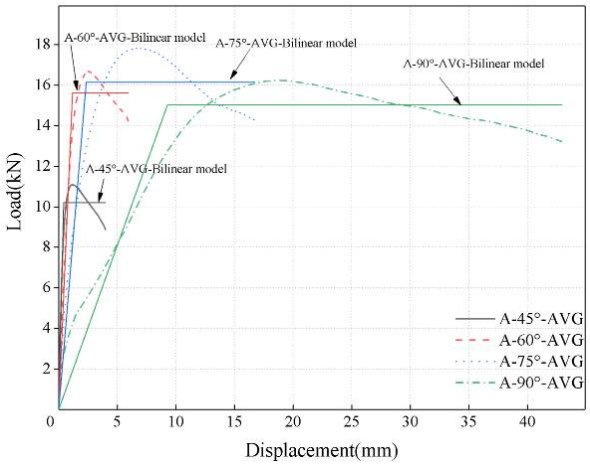

Fig. 8: The bi-linear models of specimens with different anchorage angles.

The area enclosed by the load-slip curve is the energy dissipation of this joint during the test. In terms of energy dissipation, as the anchorage angle of the self-tapping screw increases, the energy dissipation of the joint increases. In order to show this difference, the initial stiffness, yield load, ductility coefficient and energy dissipation of the joints were calculated quantitatively by pick point software (Karube et al. 2001).

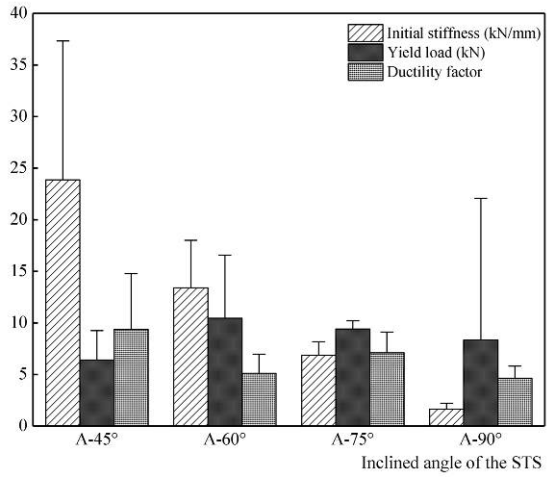

Fig. 9: The properties of specimens with different anchorage angles.

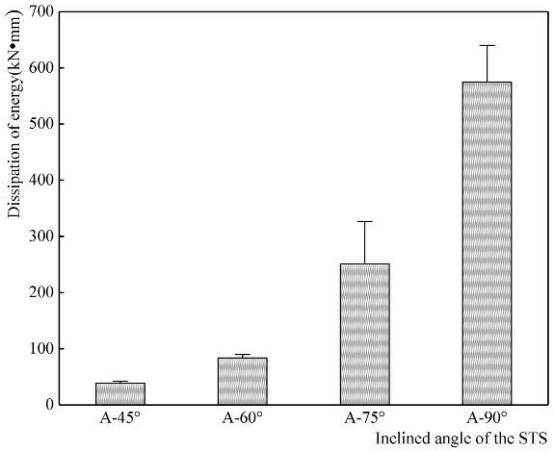

Fig. 10: The dissipation of energy of specimens with different anchorage angles.

Tab. 2: The characteristic parameter of specimens with different anchorage angles.

Anchorage angles test ID	Maximum load (kN)	Initial stiffness ($kN \cdot mm^{-1}$)	Yield load (kN)	Ductility factor	Dissipation of energy (kN·mm)
A-45°-AVG	11.09 (±1.16)	23.87 (±13.44)	6.40 (±2.84)	9.37 (±5.41)	38.65 (±3.71)
A-60°-AVG	16.70 (±1.00)	13.38 (±4.62)	10.45 (±6.11)	5.10 (±1.85)	84.00 (±5.81)
A-75°-AVG	17.83 (±1.28)	6.84 (±1.32)	9.40 (±0.80)	7.09 (±2.03)	250.96 (±75.50)
A-90°-AVG	16.23 (±0.94)	1.62 (±0.58)	8.31 (±13.76)	4.62 (±1.19)	574.76 (±65.29)

Note: The standard deviation of the six specimens in the brackets.

The load-displacement diagram was fitted by the bilinear model using EEEP method, then extract all kinds of properties of this connection draw the bar chart as Fig. 9 and Fig. 10. As Fig. 9 demonstrated that with the increase of self-tapping screw angle, initial stiffness is on the decline. In Tab. 2, the average of the initial stiffness of the specimen A-45° is 23.87 $kN \cdot mm^{-1}$. The average of the initial stiffness of the specimen A-60° is 13.38 $kN \cdot mm^{-1}$ compared with the A-45° which was reduced 43.9%. The average of the initial stiffness of the specimen A-75° is 6.84 $kN \cdot mm^{-1}$. Compared with the A-45° that was reduced 45%. The average of the initial stiffness of the specimen A-90° is 1.62 $kN \cdot mm^{-1}$, which is only 6.8% of the average initial stiffness at A-45°. That means the initial stiffness is inversely proportional to the anchorage angle. But for yielding load, the specimen of A-60° has the maximum value. In the same condition, the inclined angle 45° is always easy to yield. Compared with energy dissipation, Fig. 10 shows the trend of exponential growth, the energy dissipation is a positive correlation with anchorage angle.

When single the angle is considered changing, the effective length of self-tapping screws deep into the main material also changes. That is why the bearing capacity values of A-45° are low. On the other hand, the effective length of the embedded main wood element did no effect on the stiffness of this single shear-tension connection.

For the specimen of A-45°, with the increase in load, the self-tapping screw first bears the bending resistance of the glulam under the action of the force. When this action increases with the increase in force, the reaction force of the screw cap also increases gradually, and finally presents the failure mode of pulling out the screw. With the change of the anchorage angle, the failure mode of the specimens also changed. The specimens of A-45°and A-60° were appeared screw pulling failure, and the specimens of A-75°and A-90° showed obvious bending failure.

This phenomenon illustrates the effect of the effective length of the connector on the failure mode of the connection.

Experimental phenomena and failure modes of different anchorage angles

During the loading process, with the increase in load and displacement, this joint transitions from the elastic stage to the plastic stage. At the beginning of the yield displacement point of the specimen, the cracking occurred along with the sound. The sound is more intense near the maximum load, and the head of the screw with the angles of 75° and 90° are pulled into the lateral wood elements about 7 mm and 15 mm, respectively.

As the cross-section of the specimens in Fig. 11, the failure mode can be observed. For A-45° specimens there are no significant changes about the way of screws, but the self-tapping screw was pulled out from the main wood element. The reason is the anchorage length of the screw into the main wood element is short, which caused the effective length of the embedded main wood element was not enough. In this case, the withdraw capacity was much bigger than the yield capacity of the screw. The self-tapping screw of the A-60° specimen was bent at the shear plane, and a plastic hinge appeared. The self-tapping screws of the A-75° and A-90° specimens were bent on both sides of the connection, and two plastic hinges appeared. The bending degree of the 90° specimen was greater, and the bending

symmetrical distribution occurred at both sides of the shear plans, which resulted in the failure mode of "two-hinge yield".

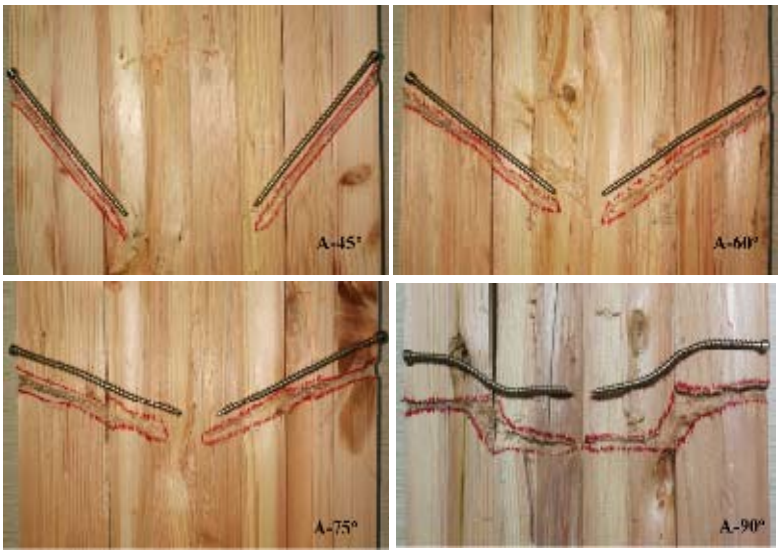

Fig. 11: Inside phenomena of different anchorage angles.

Equivalent energy elastic-plastic analysis for different edge distance

Similarly, the load-displacement diagram was fitted with a bilinear model to extract the properties of specimens with different edge distance (Fig. 12). As can be seen from Fig. 13 and Fig. 14, the initial stiffness showed an upward trend with the increase of the edge distance.

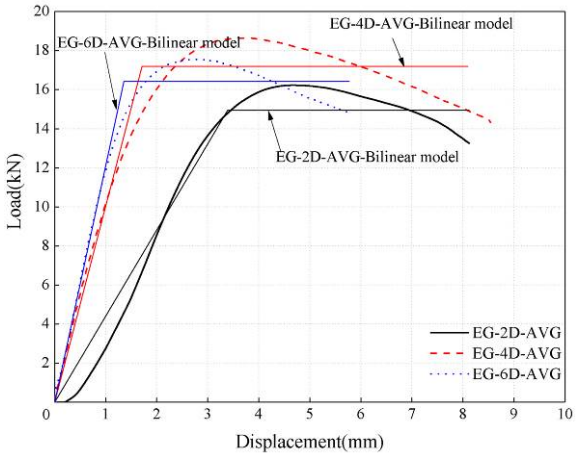

Fig. 12: The bi-linear models of specimens with different edge distances.

In Tab. 3, the average of the initial stiffness of the specimen EG-2D is 4.41 kN·mm^{-1}. The average of the initial stiffness of the specimen EG-4D is 10.04 kN·mm^{-1}. The average of the initial stiffness of the specimen EG-6D is 12.08 kN·mm^{-1}. The trend of average yield load and average ductility factor is relatively uniform, while the average energy dissipation of the specimen EG-4D is the largest (124.57 kN·mm), and the average energy dissipation of

EG-6D is the smallest (83.63 kN·mm), which decreases by 32.9% compared with the specimen EG-4D.

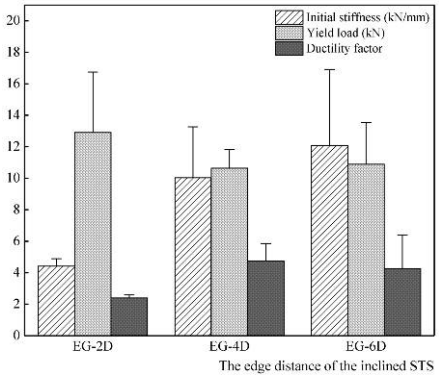

Fig. 13: The properties of specimens with different edge distances.

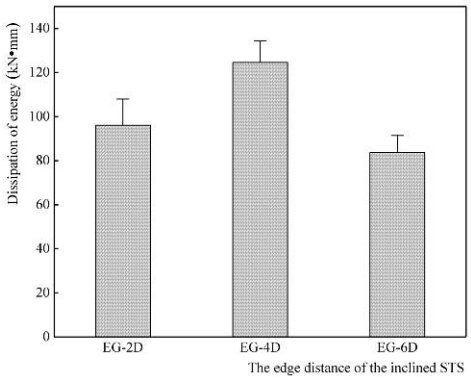

Fig. 14: The dissipation of energy of specimens with different edge distances.

Tab. 3: The characteristic parameter of specimens with different edge distances.

Edge distances test ID	Maximum load (kN)	Initial stiffness ($kN \cdot mm^{-1}$)	Yield load (kN)	Ductility factor	Dissipation of energy (kN·mm)
EG-2D-AVG	16.23 (±1.12)	4.410 (±0.48)	12.91 (±3.83)	2.40 (±0.19)	96.10 (±11.91)
EG-4D-AVG	18.65 (±1.07)	10.04 (±3.22)	10.64 (±1.17)	4.73 (±1.12)	124.57 (±9.78)
EG-6D-AVG	17.55 (±0.97)	12.08 (±4.83)	10.89 (±2.64)	4.24 (±2.15)	83.63 (±7.85)

Note: The standard deviation of the six specimens in the brackets.

Experimental phenomena and failure modes of different edge distance

During the loading process, the specimen surface has no obvious phenomenon. After unloading, the shear plane has about 2 mm gap, separated the specimen, and examined the failure modes of different edge distances. Results show that the screw was a bend in the shear plane of different edge distances and "one hinge yield" failure occurred. Moreover, these results more remarkable in the specimen EG-4D. The way of the screw and screw failure mode in the members after a load of each group of specimens was shown in Fig. 15 and Fig. 16.

Fig. 15: Inside phenomena of specimens with different edge distances.

Fig. 16: The failure mode of the self-tapping screw.

CONCLUSIONS

The push-out test was conducted with self-tapping screws at four anchorage angles (A-45°, A-60°, A-75°, and A-90°), three edge distances (EG-2D, EG-4D, and EG-6D). Using the energy elastic-plastic curve method (EEEP) method to study the effect of edge distances on stiffness and other properties of the joint.

The results showed that the anchorage angles of STS had a significant impact on the initial stiffness of this joint, with the increase of self-tapping screw angle, initial stiffness is on the decline. In terms of initial stiffness, the specimen of A-45° is 23.87 kN·mm^{-1}, but it is the easiest to buckle, and has lower energy dissipation and ductility. The maximum yield load at the specimen of A-60° is 10.45kN. For the specimen of A-45°, the stiffness of the connection is the smallest, and the energy dissipation value is the largest 574.76 kN·mm.

With the increase of the edge distances, the initial stiffness increased, and the yield load, ductility coefficient, and energy dissipation were uniform. The stiffness of specimen EG-2D is 4.41 kN·mm-1. The stiffness of specimen EG-4D is 10.04 kN·mm-1, which increases by 128% compared with the specimen EG-2D. The stiffness of specimen EG-6D is 12.08 kN·mm-1, which increases by 174% compared with the specimen EG-2D. However, the ductility coefficient, yielding load, and energy dissipating have no significant change.

Experimental results presented in this research the effect of the edge distances has a significant impact on the stiffness of the connection. The effective range of the STS has to be considered in the future test.

ACKNOWLEDGEMENTS

This paper was financially supported by the National Natural Science Foundation of China (Grant No.31670566) and the Research Project of Jiangxi Forestry Bureau (Grant No.202013). In this research, Glulam was supported by Jiangsu Huiyoulin Building Technology Co., LTD. The full thread screws provided by Shanghai More Good Fasteners Co., LTD. The authors would like to express their sincere thanks to these supports.

REFERENCES

1. ASTM F1575-17, 2017: Standard test method for determining bending yield moment of nails.
2. ASTM D1761-12, 2012: Standard test methods for mechanical fasteners in wood.
3. ASTM E2126-19, 2019: Standard test methods for cyclic (reversed) load test for shear resistance of vertical elements of the lateral force resisting systems for buildings.
4. Blass, H.J., Bejtka, I., 2001: Screws with continuous threads in timber connections. Pp 193-201, Proceedings PRO 22. International RILEM symposium on joints in timber structures. Stuttgart, Germany.
5. Bejtka, I., Blass, H.J, 2002: Joints with inclined screws. Pp 141-154, In: Meeting, international council for research and innovation in building and construction working commission W18-timber structures. Kyoto, Japan. (Paper No. CIB-W18/35-7-4).
6. Brandner, R., Ringhofer, A., Grabner, M., 2018: Probabilistic models for the withdrawal behavior of single self-tapping screws in the narrow face of cross laminated timber. European Journal of Wood Products 76: 13–30.
7. Chang, C., Fang, Y.F., Liu, Y.F., Que Z.L., 2019: Study on pull-out performance of tilted self-tapping screw in cross-laminated timber. Architecture Technology 50(04): 416-418. (In Chinese)
8. Chen, Z.Y., Wang, X.M., Dang, W.J., Dong, L., Chen, J., Que, Z.L., 2020: Study on performance of steel-to-timber joints with inclined self-tapping screws for cross-laminated timber structures. Architecture Technology 51(03): 288-291. (In Chinese).
9. Dietsch, P., Brandner, R., 2015: Self-tapping screw and threaded rods as reinforcement for structural timber elements. A state-of-the-art report. Construction and Building Materials 97: 78-89.
10. EN 1995-1-1, 2009: Eurocode 5: Design of timber structures part 1-1: general-common rules and rules for buildings.
11. Girhammar, U.A., Nicolas J., Bo, K., 2017: Stiffness model for inclined screws in shear-tension mode in timber-to-timber joints. Engineering Structures 136: 580-595.
12. GB 50005-2017, 2017: The standard for the design of timber structures. (In Chinese)
13. Johansen, K., 1949: Theory of timber connection. Bridge Structural Engineering 9: 249-262.
14. Jockwer R., Steiger R., Frangi A., 2014: Design model for inclined screws under varying load to grain angles. Pp 141-153, Meeting 47 of the International Network for Timber Engineering Research INTER. Bath, United Kingdom. (Paper No. INTER/47-7-5).
15. Komatsu, K., Teng, Q.C., Li, Z.R., Zhang, X.L., Que Z.L., 2019: Experimental and analytical investigation on the nonlinear behaviors of glulam moment-resisting joints composed of inclined self-tapping screws with steel side plates. Advances in Structural Engineering 22(15): 3190-3206.
16. Karube, M., Harada, M., Hayashi, T., 2001: A proposal of bi-linear modeling tool for assess its method and problem in common tool for load-deformation curves of wooden

structures. Digests of Annual Meeting of Architectural Institute of Japan C-1(3): 215-216. (In Japanese).
17. LY/T 2377, 2014: Test methods for the joint performance with dowel type fasteners used in wooden structural material (In Chinese).
18. LY/T 2056, 2012: Steel nails for timber structures (In Chinese).
19. Lu, X.R., Teng, Q.C., Li, Z.R., Zhang, X.L., Wang, X.M., Komatsu, K., Que, Z.L., 2020: Study on shear property of spruce glulam and steel plate connected with inclined screw. Journal of Forestry Engineering 5(3): 48-53. (In Chinese).
20. Que, Z.L., Han, C., Teng, Q.C., Hu, C.S., Luo, W.S., 2020: Study on anti-side performance of glulam beam-column joints with inclined screw. China Forest Products Industry 57(05): 34-40. (In Chinese).
21. Ringhofer, A., Brandner, R., Schickhofer, G., 2015: Withdrawal resistance of self-tapping screws in unidirectional and orthogonal layered timber products. Materials and Structures 48: 1435–1447.
22. Symons, D., Persaud, R., Stanislaus, H., 2010: Slip modulus of inclined screws in timber-concrete floors. Structures and Buildings 163(4): 245–55.
23. Teng, Q.C., Wang, F.B., Que Z.L., Zeng, N., 2020: Effects of angles on the screw and nail withdrawal strength in dimension lumber. Scientia Silvae Sinicae 56(01): 154-161.
24. Tomasi, R., Crosatti, A., Piazza, M., 2010: Theoretical and experimental analysis of timber-to-timber joints connected with inclined screws. Construction and Building Materials 24(9): 1560-1571.
25. Williams, M., Mohammad, M., Alexander, S., Pierre, Q., 2008: Determination of yield point and ductility of timber assemblies: In search for a harmonized approach. Pp 1064-1071, 10th World Conference on Timber Engineering, Miyazaki, Japan.
26. Wang, F.B., Wang, X.M., Cai, W.Z., C., Chang, C., Que Z.L., 2019: Effect of inclined self-tapping screw connecting laminated veneer lumber on the shear resistance. Bioresources 14(2): 4006-4021.
27. Yang, X.J., Ma, L., Que Z.L., Yu, Y.H., 2018: Enduring performance of self-tapping screw connection in wood members and WPC members. Wood Research 63(5): 833-842.
28. Yang, R.Y., Zhang X.F., Yuan Q., Sun Y.F., Wu Y.H., 2020: Research of pin slot embedding yield strength parallel to grain of *Larix gmelinii*. Journal of Forestry Engineering 5(05): 131-138.
29. Zhang Y., Liu X.Y., Hu Q.B., Gao Y., 2019: Influence of old panel on the mechanical properties of nailed joints in light wood frame structure. Journal of Forestry Engineering 4(01): 51-58.

YIFAN LIU, ZIYIN YAO, ZELI QUE*
NANJING FORESTRY UNIVERSITY
COLLEGE OF MATERIALS SCIENCE AND ENGINEERING
NANJING 210037
P.R. CHINA
*Corresponding author: zelique@njfu.edu.cn

FEIBIN WANG
NANJING FORESTRY UNIVERSITY
COLLEGE OF LANDSCAPE ARCHITECTURE
NANJING 210037
P.R. CHINA

HUI HUANG
JIANGXI ACADEMY OF FORESTY
INSTITUTE OF FOREST PRODUCTS INDUSTRY
NANCHANG 330032
P.R. CHINA